Effect of reaction steps and disolved nitrogen on the oxy-combustion and emission characteristics inside an industrial water tube boiler

*Rached Ben-Mansour[1), 2)] Mohamed A. Habib[1)], Mohamed Rajhi[1)],
Medhat A. Nemitallah[1)], Kabir A. Suara[1)]

[1)] *Department of Mechanical Engineering,*
King Fahd University of Petroleum & Minerals, Dhahran 31261, Saudi Arabia.
[2)] *rmansour@kfupm.edu.sa*

ABSTRACT

In the present research work, numerical investigations on the effect the number of reaction steps on the oxy-combustion characteristics inside an industrial furnace of a water tube boiler are conducted. Furthermore, the influence of oxygen impurities on the temperature and NO_x formation of oxyfuel combustion in the same furnace is studied and the results are presented in this paper. Validations of the present computational model were performed by comparing the predicted results with the experimental data and showed a good agreement between predicted and experimental data. The calculations were made for different N_2 percentage of 0, 2, 4 and 6%. Two reaction models were utilized. The first is a one-step and the second is a two-step reaction. The results provide influence of oxygen impurities on the temperature inside the furnace. They also provide influence of N_2 on the maximum temperature, total and thermal NO_x. As the carbon dioxide is reduced and nitrogen is introduced, the temperature levels are found to be reduced. The thermal NO is shown to increase with N_2%. At the exit section, Thermal as well as prompt NO increase as N_2 value rises. The results show that increasing the percent of the CO_2 in the CO_2-O_2 side mixture results in a reduction in both the total and radiation heat flux. The change of the reaction model to double-step reactions results in slight reduction in the fluxes which may be attributed to the incomplete combustion of the fuel.

1. INTRODUCTION

As energy use grows, concerns over global warming may lead to imposing limits on greenhouse gas emissions from fossil fuel plants. This has stimulated extensive research on the subject of carbon capture and sequestration. To achieve a deep reduction in carbon dioxide emissions through carbon capture and sequestration within power generation systems, several technologies are being investigated. The considered technologies for the reduction of carbon dioxide, CO_2, emissions from power plants include post-combustion, pre-combustion, and oxy-fuel combustion technologies (IPCC 2007, Ghoniem 2011). In oxy-fuel combustion, fuels are burned in a nitrogen-lean and carbon dioxide-rich environment, which is achieved by feeding the

combustor with an oxygen-rich stream and recycled flue gases. The characteristics of oxyfuel combustion and air-fuel combustion in the furnace of a typical industrial water tube boiler using methane as the operating fuel were investigated numerically by Ben-Mansour *et al.* (2012, 2014). In this study, two oxyfuel cases were considered and the analysis was conducted for two oxy-fuel cases that correspond to 21% O_2 (by volume) and 29% O_2 in the oxidizer mixture ($O_2 + CO_2$). The results showed that the temperature levels are greatly reduced as the percentage of recirculated CO_2 is increased. They concluded that the flame propagation speed in CO_2 environment is lower than that in N_2. Compared to conventional air combustion, oxyfuel combustion shows different characteristics of heat transfer, ignition as well as NO_x emission.

Shah and Kristie (2007) made a comparison between the performance of boilers utilizing oxyfuel combustion and air combustion and reported an efficiency reduction and a reduction of CO_2 emission. This reduction in efficiency is due to penalty of separating oxygen and the reduction of CO_2 emissions is because of its recirculation in combustion from the exhaust gases and the capture of the most of CO_2 out in the exhaust. The impact of oxy-combustion on the design of heat exchange surfaces was investigated by Kakaras *et al.* (2007) and it was found that higher radiative heat transfer. They contributed this to the high concentrations of CO_2 and H_2O in the flue gas. Andersson *et al.* (2009) compared the radiative heat transfer in oxy-fuel flames to corresponding conditions in air-fuel flames during combustion of lignite in the Chalmers 100 kW oxy-fuel test facility. In their study, they found that the temperature, and thereby the total radiation intensity of the oxy-fuel flames, increases with decreasing flue-gas recycle rate. Also, the ratio of gas and total radiation intensities was increased under oxy-fuel conditions compared to air-firing. Andersson and Johnsson (2008) compared radiative heat transfer in oxyfuel flames and air-fuel flames during combustion of lignite. In another study, Andersson *et al.* (2009) presented their results on the differences in soot-related radiation intensity between two different oxyfuel flame and air-fired flame. The fundamentals of the oxyfuel combustion for gas and coal firing in a 100 kW oxyfuel test facility were studied experimentally and theoretically by Andersson (2006). The results showed that the temperature level of the flame (using 27% O_2 and 73% CO_2 and a swirl number of 0.79) drops drastically and leads to a delayed burn-out compared to the normal air-fuel flames. Shaddix (2007) studied the combustion behavior and ignition of individual coal particles in 6-36% O_2 in N_2 and in CO_2 at 1400 to 1800 K. Similar results have been found in other experimental and theoretical investigations of oxyfuel flames (Wall *et al.* 2007). Ditaranto and Hals (2007) showed that additional control of CO_2 dilution/ O_2 enrichment allows more possibilities for "zoning" the flame.

CFD techniques have become significantly important in fluid dynamics and combustion studies alongside analytical modeling and experimental diagnostics. CFD provides a relatively inexpensive and indispensable tool to perform comprehensive studies on the fluid flow, heat transfer and chemical reactions in combustion (Chen *et al*. 2012). With the accumulated knowledge from the literature work on the fundamental differences between air-fuel and oxy-fuel combustion, some effort has gone into developing and validating sub-models for the new combustion environment (Chen and Ghoniem 2012). The number of reaction steps is one of the most important parameters in turbulent combustion modeling, because of its role in establishing the reaction rates, species concentrations and combustion temperature inside the reactor. In the present

research work, numerical investigations on the effect the number of reaction steps on the oxy-combustion characteristics inside an industrial water tube boiler are conducted. The effect of dissolved nitrogen in the oxygen supplied for combustion on the combustion and emission characteristics is also investigated.

2. MATHEMATICAL FORMULATIONS

2.1 The Governing Equations

The mathematical model is based on the numerical solution of the conservation equations for mass, momentum, and energy, and transport equations for scalar variables. The equations, which are elliptic and three-dimensional, were solved to provide results of the flow pattern, thermal and emissions characteristics of reacting medium inside a boiler furnace. The present work utilizes the K-ε model of Versteeg and Malalasekera (1995). The Reynolds stresses and turbulent scalar fluxes are related to the gradients of the mean velocities and scalar variable, respectively, via exchange coefficients as follows (Wilcox 2000)

$$-\rho \overline{u_i u_j} = \mu_t \left(\frac{\partial \overline{U}_i}{\partial x_j} + \frac{\partial \overline{U}_j}{\partial x_i} \right) - \frac{2}{3} \rho k \delta_{ij} \tag{1}$$

$$-\rho \overline{u_j \phi} = \Gamma_\Phi \frac{\partial \Phi}{\partial x_j} \tag{2}$$

where: μ_t is the turbulent viscosity and Γ_Φ is equal to μ_t / σ_Φ. The turbulent viscosity is modeled as

$$\mu_t = c_\mu \rho k^2 / \varepsilon \tag{3}$$

where c_μ and σ_Φ are constants. The turbulent viscosity is thus obtained from the solution of the transport equations for K and ε. Renormalized group turbulence model (Wilcox 200) was used to provide better results for vertical flows. The eddy dissipation model (Magnussen and Hjertager 1976) and the discrete ordinates (DO) radiation model (Raithby and Chui 1990) were used to provide the production rate of species and the radiation heat transfer. The blackbody spectral emissive power is calculated using variables by Liu *et al*. (1998) and Zheng *et al*. (2000) based on expressions of Modak (1979) and Smith *et al*. (1982).

2.2 Species Transport Equations

The mass fraction of each species m_l, is predicted through the solution of a convection-diffusion equation for the lth species. The present calculations utilize a one-

step reaction model and solve transport equations for the species of O_2, CO_2 and H_2O. The conservation equations can be expressed in the following form:

$$\frac{\partial}{\partial x_i}(\rho \overline{U}_i m_l) = -\frac{\partial}{\partial x_i} J_{l,i} + R_l \tag{4}$$

where R_l is the mass rate of creation or depletion by chemical reaction of the species I, $J_{l,i}$ is the diffusion flux of species I, which arises due to concentration gradients which is given by

$$J_{l,i} = -(\rho D_{l,m} + \frac{\mu_t}{Sc_t})\frac{\partial m_l}{\partial x_i} \tag{5}$$

where $D_{l,m}$ is the diffusion coefficient for species I in the mixture and Sc_t is the turbulent Schmidt number, $\frac{\mu_t}{\rho D_t}$ is equal to 0.7. An eddy-dissipation model (Magnussen and Hjertager 1976) that relates the rate of reaction to the rate of dissipation of the reactant- and product-containing eddies is used to calculate the rate of reaction.

2.3 Radiation Heat Transfer Modeling

In order to correctly predict the temperature distribution in the furnace a radiative transfer equation (RTE) for an absorbing, emitting and scattering medium has to be solved. The RTE equation is written as

$$\frac{dI(\mathbf{r},\mathbf{s})}{ds} = \kappa I_b - (\kappa + \sigma_s)I(r,s) \tag{6}$$

The total radiation intensity I, depends on the position vector, r, and the path length s. κ is the absorption coefficient and σ_s is the scattering coefficient. The Planck mean absorption coefficient is given as

$$\kappa_P(T,P) = \frac{\int_0^\infty \kappa_\lambda(\lambda,T,P)e_{b\lambda}(\lambda,T)d\lambda}{\sigma T^4} \tag{7}$$

where $e_{b\lambda}$ is the blackbody spectral emissive power. κ is calculated using variables by Liu *et al.* (1998) based on expressions reported by Modak (1979). An accurate calculation of the gas radiation property must consider the spectral absorption of CO_2 and H_2O, and also the overlap between these radiating gas components. Since direct prediction of the absorption coefficient is computationally complex, models for absorption properties, such as the gray gas, will have to be employed in the radiation heat transfer model. The most commonly used gray gas model in CFD is the weighted sum of gray gases (WSGG) model proposed by Smith et al. (1982) has been applied in the present CFD calculations. In this model, the gas is assumed to consist of a transparent gas and several gray gases without any wavelength dependence, and the model parameters are based on the radiation properties of air-fired flue gases.

2.4 Reaction kinetics models

2.4.1 Single step model
The simplest oxidation mechanism assumes that products of the chemical reaction consist only of CO_2 and H_2O

$$CH_4 + 2O_2 \rightarrow CO_2 + 2H_2O \qquad (8)$$

The physical situation that this assumption reasonably approximates a diffusion flame suspended in the flow field at relatively high temperature (Mancini and Mitsos 2011). Here, the oxygen diffuses across the boundary layer to meet methane in a small, well-defined reaction zone. The high temperature of the flame accelerates the local homogeneous kinetics, and mostly produces CO_2 and H_2O only, if the flame temperature is not too high. However, for the purposes of the present model, we need only to show that the reaction rates are so much fast that chemical equilibrium is always locally attained. Finally, it is assumed that the homogeneous gas phase reactions in the relatively cool bulk are so slow that once the products of the reaction have formed and leave the reaction zone back to the free stream, they do not have a sufficient residence time to interact and form species such as H_2 or CO.

2.4.2 Two step model
As a matter of fact, numerical modeling of combustion applications is a computationally demanding process. That's why it is necessary to apply simplified reaction mechanisms to reduce the computing cost. Examples of CFD modeling in combustion application using the global mechanisms are found in the literature (Brink et al. 2000, Saario and Oksanen 2008). However, computationally simple mechanisms are cheap, simple and available; the simplified schemes cannot be expected to give accurate results especially under oxy-fuel combustion conditions. The replacement of inert N_2 with a chemically reactive compound, CO_2, has been shown to change the importance of some of the elementary reactions governing the combustion, thereby requiring a modification of the global multistep reaction mechanisms to make them valid under oxy-fuel conditions (Glaborg and Bentzen 2007). In the present work, the two-step hydrocarbon oxidation mechanism by Westbrook and Dryer (1981) which was modified by Andersen et al. (2009) is used for the calculations of the reaction kinetics, since this scheme is directly available as default in the commercial CFD code Fluent. The model was modified to handle the increased CO_2 concentration under oxy-fuel conditions. Westbrook and Dryer included the reverse reaction step for CO_2 decomposition in order to reproduce the proper heat of reaction and pressure dependence of the [CO]/[CO$_2$] equilibrium. The mechanism of Westbrook and Dryer (1981) consists of two step reactions with the second step oxidation of CO to CO_2, is only reversible. The two step reaction kinetics model has been considered in this work for simplification of the reactions kinetics calculations with reasonable results regarding the species concentrations as compared to the detailed model (Andersen et al. 2009). The mechanism is listed in the form of three irreversible steps

$$CH_4 + 1.5O_2 \quad \rightarrow \quad CO + 2H_2O \qquad\qquad \text{reaction 1} \qquad (9)$$

$$CO+0.5O_2 \rightarrow CO_2 \qquad\qquad \text{reaction 2} \qquad (10)$$

$$CO_2 \rightarrow CO+0.5O_2 \qquad\qquad \text{reaction 3} \qquad (11)$$

For this model, the modified reactions rates data by Andersen et al. (2009) are listed in Table 1. The set of governing equations and boundary conditions are solved numerically. The details of the calculation procedure can be found in previous works (Habib *et al*. 2012).

2.5 Boiler description

In the present research work, numerical investigations on the effect the number of reaction steps on the oxy-combustion characteristics inside an industrial water tube boiler are conducted. The effect of dissolved nitrogen in the oxygen supplied for combustion on the combustion and emission characteristics is also investigated. Fig. 1 shows the Cartesian coordinate system of the boiler furnace that is used in this study.

Table1 Modified two-Step Methane-oxygen Combustion Mechanisms with Kinetic Rate Data [29]

| Reaction number	Reactions	A	β	E_a(J/kmole)	Reaction orders
Reaction 1	$CH_4+1.5O_2 \rightarrow CO+2H_2O$	$1.59*10^{13}$	0	$1.998*10^8$	$[CH_4]^{0.7}[O_2]^{0.8}$
Reaction 2	$CO+0.5O_2 \rightarrow CO_2$	$3.98*10^8$	0	$4.18*10^7$	$[CO][O_2]^{0.25}[H_2O]^{0.5}$
Reaction 3	$CO_2 \rightarrow CO+0.5O_2$	$6.16*10^{13}$	-0.97	$3.277*10^8$	$[CO_2][H_2O]^{0.5}[O_2]^{-0.25}$
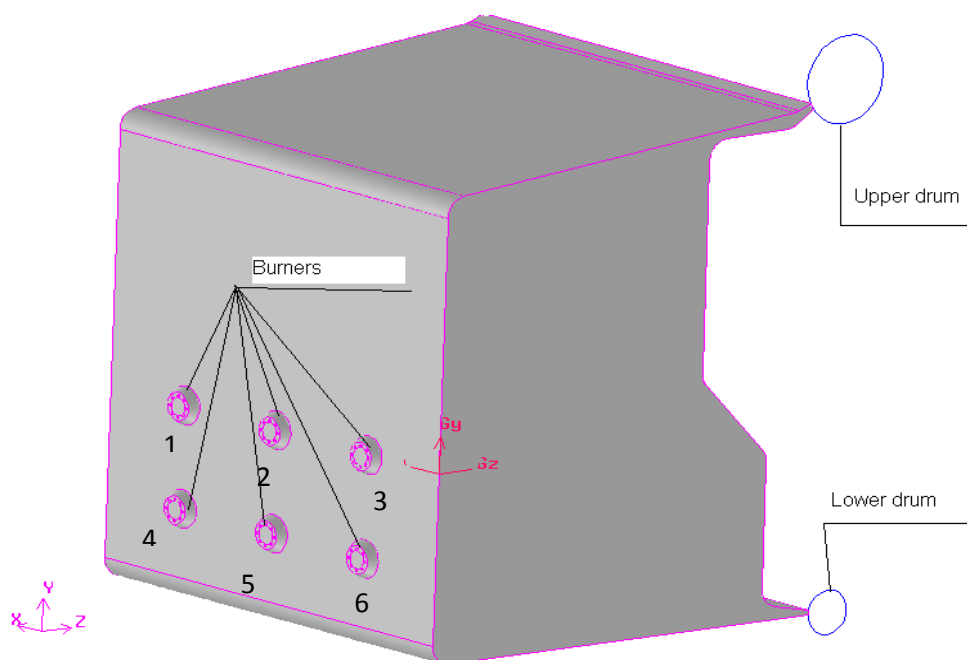
Fig. 1 Three-dimensional view of a typical package boiler

The boiler uses natural gas as a fuel and has 6 burners on two levels (three burners in each level) located in the front wall (burner wall). The D-type tubes extend from the mud drum (lower drum) through the bottom wall and form the burner wall. The top part of the D-shaped tubes forms the top wall of the furnace and ends at the upper drum. The tubes forming the bottom wall are thermally insulated. Tubes on the front wall extend from lower to upper drum while the tubes forming the side walls extend from a lower header to an upper header. The water-steam mixture inside the tube is normally saturated and has a fixed saturation temperature corresponding to the drum pressure. Accordingly, the front, side, rear and top walls of the furnace provide a constant temperature boundary condition. The fuel is introduced through the nozzles surrounded by the primary air. The primary air is given a tangential component using 45° swirl angle (equivalent to swirl number of 0.58). The secondary air flows around the primary air nozzles with no swirl component. The mass flow rates of the primary and secondary air streams are 8.86 and 10.6 kg/sec, respectively. The boiler has a firing rate of 298 MW with a drum pressure of 52 atm. and steam flow rate of 94.7 kg/s.

2.6 Boundary Conditions and solution procedure

Uniform velocity distribution is assumed at the inlet section. Kinetic energy and its dissipation rate are selected such that $\sqrt{K/\overline{U}^2} = 0.1$. A length scale, *L*, equal to the characteristic length of the inlet pipe/annulus is considered. At the wall boundaries, all velocity components are set to zero. Constant wall temperature corresponding to saturated water temperature in the tube wall of the actual boilers was considered. This assumption is made based on using higher thermal conductivity material that enables the release of its heat to the water that is in contact with this material. And also the thickness of this material is assumed to be very small. The production of kinetic energy and its dissipation rate at the wall-adjacent cells are computed on the basis of the local equilibrium hypothesis. Under this assumption, the production of k and its dissipation rate are assumed to be equal in the wall-adjacent control volume. The ε-equation is not solved at the wall-adjacent cells. Thus, the production of k at the node close to the wall is taken proportional to the square of the wall shear stress. The rate of dissipation, ε, at the node close to the wall is proportional to $k^{3/2}$ (Versteeg and Malalasekera 1995). The set of governing equations and boundary conditions are solved numerically. The details of the calculation procedure can be found in previous works (Ben-Mansour et al 2014). A mesh of more than 1,000,000 tetrahedral finite volumes was used. The solution was considered converged when the summation of the residual in the governing equation summed at all domain nodes was less than 0.01%. In order to minimize the errors due to false diffusion, the grids were concentrated in the regions of high gradients. The solution procedure solves the partial differential equations for conservation of mass, momentum and energy and combustion species.

3. RESULTS

3.1 Model validation

Validations of the present computational model were performed by comparing the predicted results with the experimental data of Andersson and Johnsson (2007). The combustion chamber in this case is shown in Fig. 2. Fuel is introduced in the central jet, surrounded by two annular oxidizer jets, a primary stream and a secondary stream. Both streams could be subjected to swirl, as described next. The oxidizer streams were either air for the case of air based combustion or a mixture of CO_2 and O_2 for the case of oxyfuel combustion. The operating parameters are given below in Table 2.
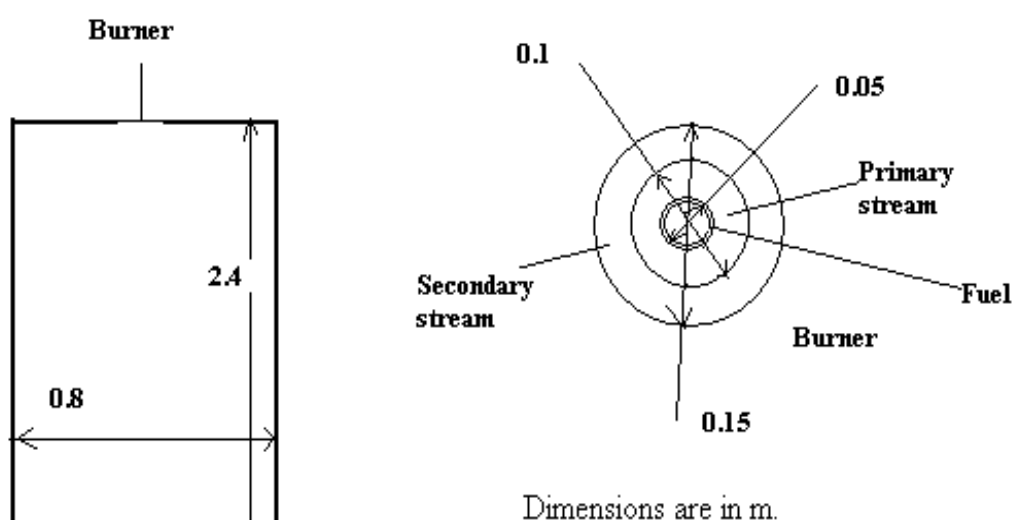
Fig. 2 Experimental O_2/CO_2 combustion Unit (Andersson and Johnsson 2007)

Table 2 Experimental Validation Furnace Operating conditions, Andersson and Johnsson (2007)

Fuel:	
Type	*Propane*
Mass flow rate	*0.001726kg/s*
Inlet Temperature	*300K*
Oxidant Stream – Case A	
Primary Stream	Air
Mass flow rate	*0.0126 kg/s*
Swirl Angle	*45°*
Inlet Temperature	*300K*
Secondary Stream	Air
Mass flow rate	*0.0188 kg/s*
Swirl Angle	*15°*
Inlet Temperature	*300 K*
Oxidant Stream – Case B	
Primary Stream	O_2, 21%; CO_2, 79% by volume
Secondary Stream	O_2, 21%; CO_2, 79% by volume
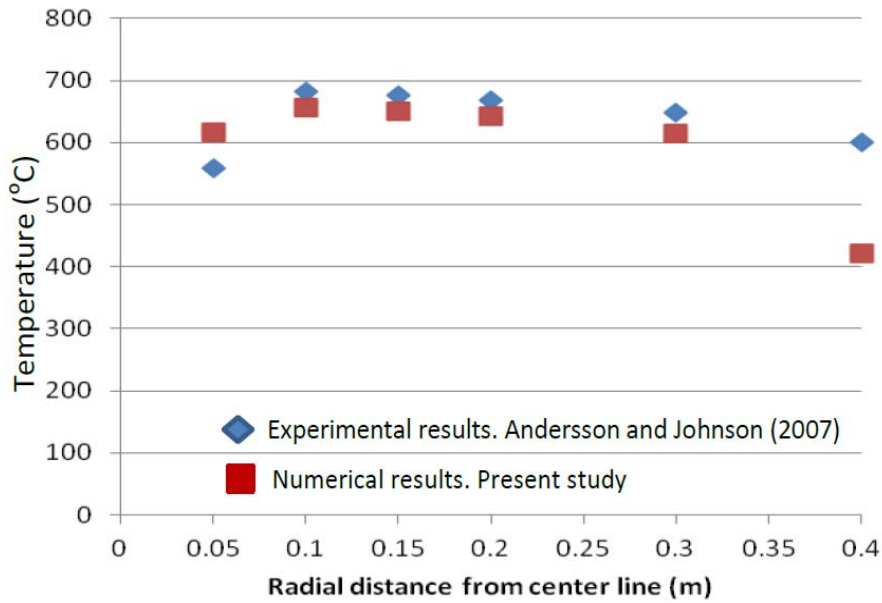
Fig. 3 Experimental vs. numerically predicted temperature profiles
at distance 0.046 m from burner for oxyfuel OF21 case

The radial temperature profiles at 0.046 m shown in Fig. 3 for oxyfuel-based combustion case show a good agreement between predicted and experimental data, although few measurements are available.
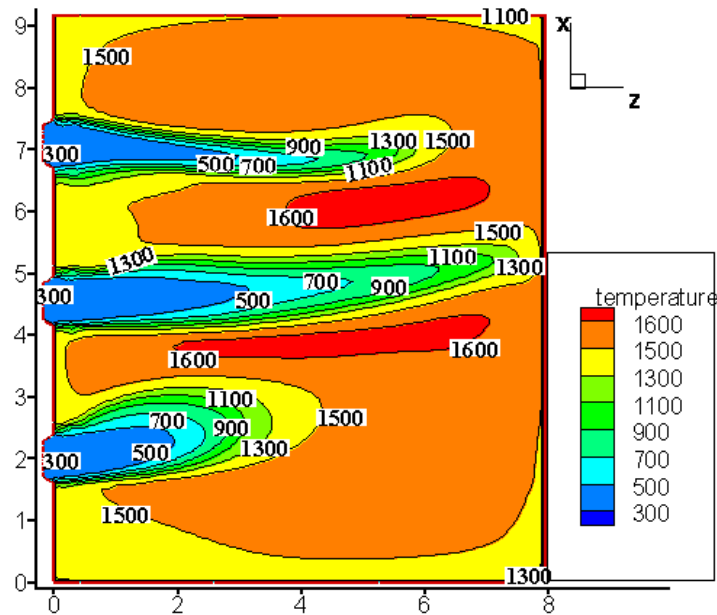

Fig. 5 Contours for temperature (K) of horizontal plane passing through burners
4, 5 & 6 for oxyfuel combustion (29% O2 and 71% CO2 by volume)

224

3.2 Influence of oxygen impurities

The influence of oxygen impurities on the temperature and NO_x formation of oxyfuel combustion in an industrial furnace is studied and the results are presented in this section. The calculations were made for different N_2% of 0, 2, 4 and 6%. Two reaction models are utilized. The first is a one-step and the second is a two-step reaction. The results provide influence of oxygen impurities on the temperature inside the furnace.
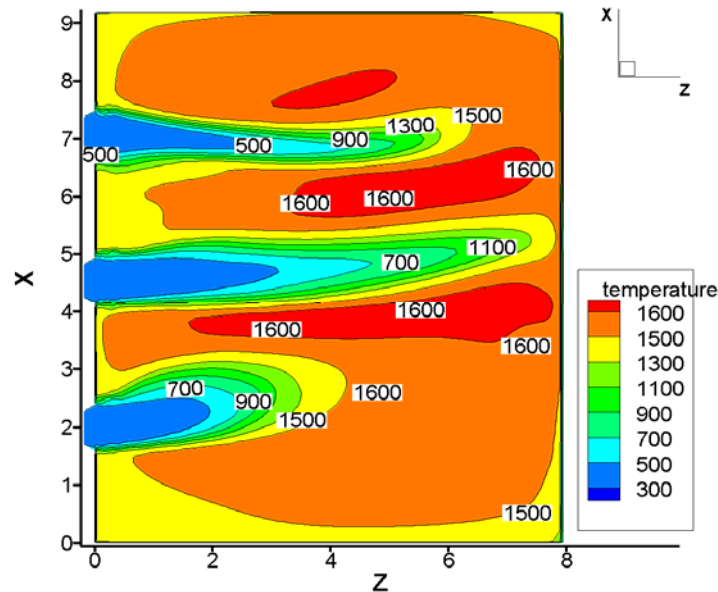

Fig. 6 Contours for temperature (K) of Lower horizontal plane
for oxyfuel combustion (29%O2, 69% CO2 and 2% N_2 by volume)
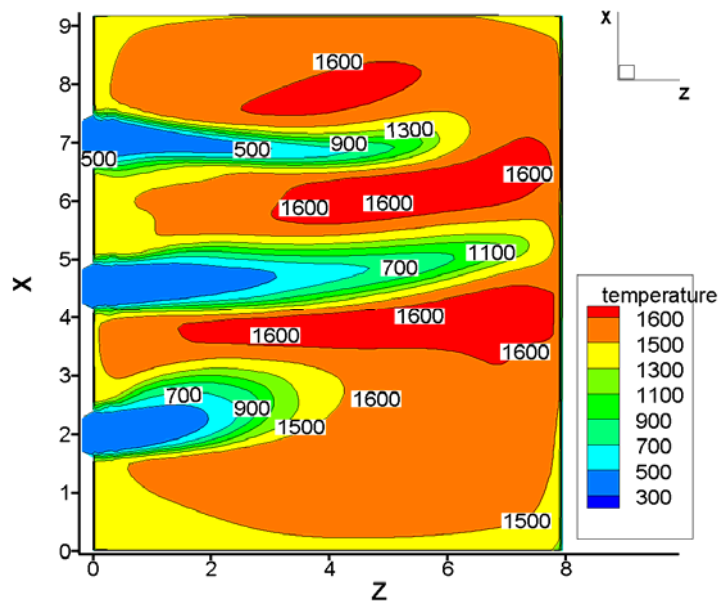
Fig. 7 Contours for temperature (K) of Lower horizontal plane
for oxyfuel combustion (29%O2, 67% CO2 and 4% N_2 by volume)

225

They also provide influence of N_2 on the maximum temperature, total and thermal NO_x. The results are obtained for different planes which include the vertical plane passing through the two burners and on two horizontal planes passing through each of the two burners. Fig. 5 presents the temperature distribution along a vertical plane passing through the three burners for the case of oxyfuel combustion with 100% pure oxygen. As shown, the flame interactions lead to higher temperature at the interface between the flames. As the carbon dioxide is reduced and nitrogen is introduced, Fig. 6, the temperature levels are found to be reduced. As the nitrogen percent is further
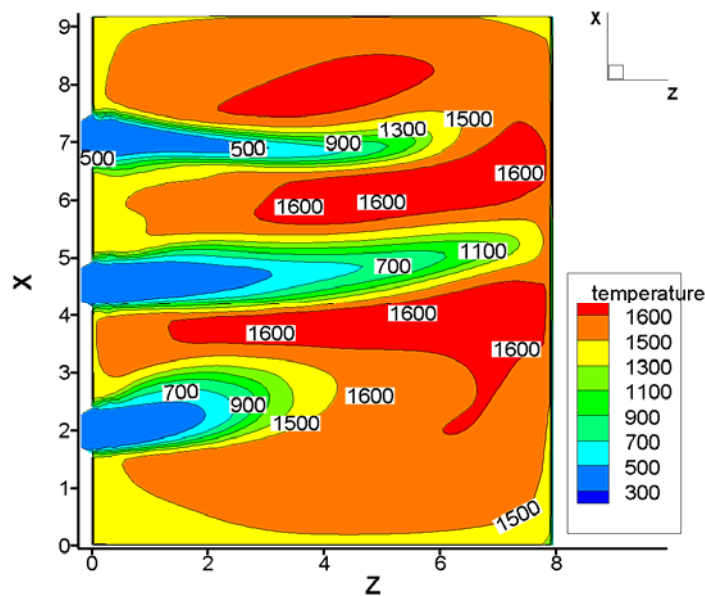
Fig. 8 Contours for temperature (K) of Lower horizontal plane for oxyfuel combustion
(29% O2, 65% CO2 and 6% N_2 by volume)
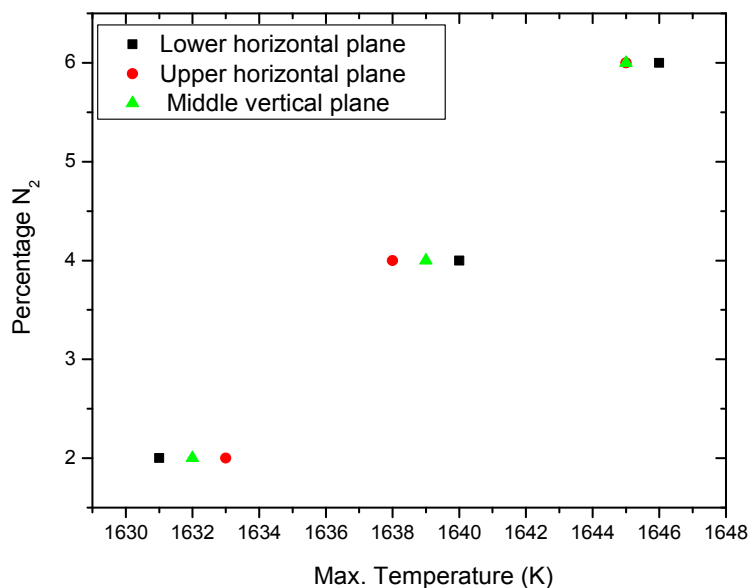
Fig. 9 Influence of the oxygen impurities on the maximum values of the temperature

226

increased, Figs. 7 and 8, to 4% and 6% the temperature levels increases slightly as can be indicated by the regions occupied by the temperature 1600 K.

The influence of the nitrogen percent in the inlet flow (oxygen impurities) on the maximum temperature and on total and thermal NO_x as well as NO concentration at the exit plane are presented in Figs. 9-12. Fig. 9 shows that the maximum temperature increases with rise in N_2% for all presented planes. The total NO_x increases with rise in N_2% for all presented planes as shown in Fig. 10. The thermal NO_x, Fig. 11, is shown to increase with N_2% for all of the three plane cases. At the exit section, Fig. 12, NO increases as N_2 value rises as well the prompt NO_x is high.
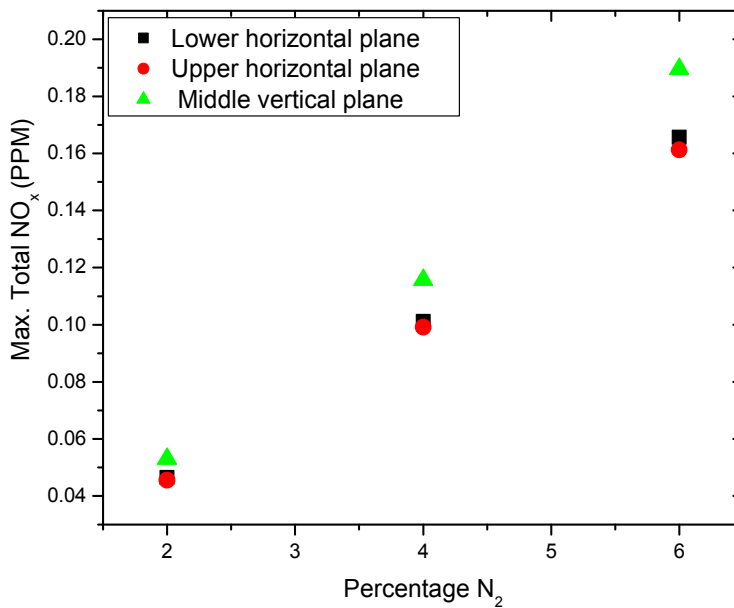

Fig. 10 Influence of the oxygen impurities on the maximum values of the total NO_x
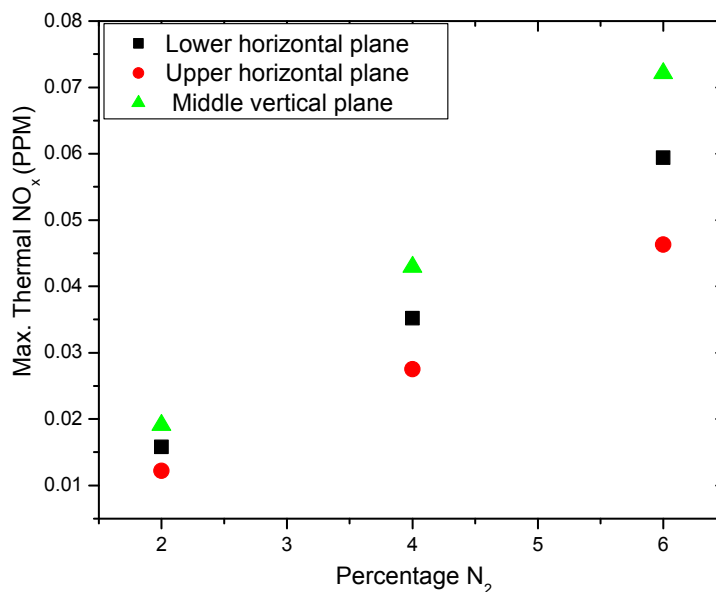

Fig. 11 Influence of the oxygen impurities on the maximum values of the thermal NO_x

227
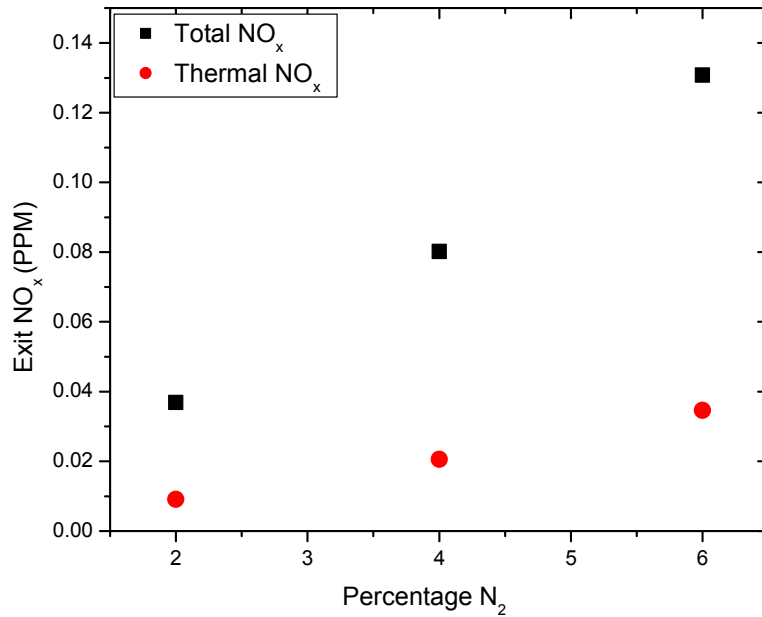
Fig. 12 Influence of the oxygen impurities on the total NO_x at the exit plane
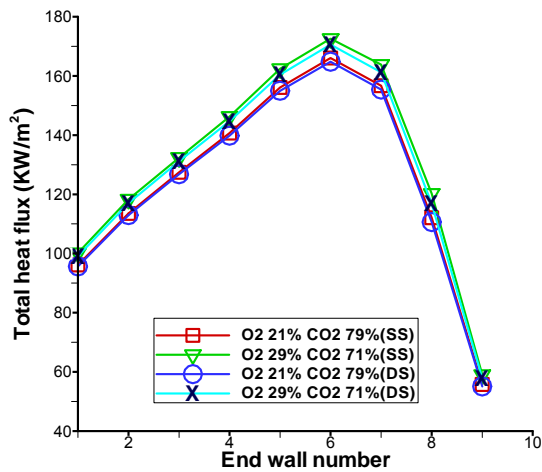

Fig. 13 Total heat flux along the end wall
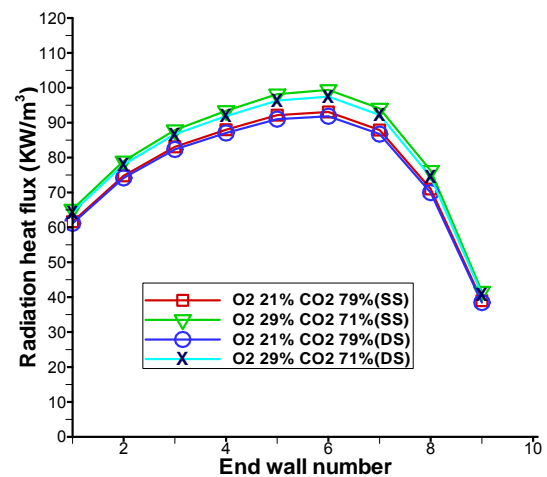
Fig. 14 Radiation heat flux along the end wall

3.3 Influence of CO_2 circulation and reaction model

Figs. 13-18 present the total and radiation heat flux along the end, front, and top and considering two-step reaction models. Figs. 13 and 14 present the total and radiation heat flux along the end wall and provides a comparison of the different cases of O_2% and the two cases of reaction model. The figures show that increasing the percent of the CO_2 in the CO_2-O_2 side mixture results in a reduction in both the total and radiation heat flux. This is attributed to the high thermal capacity of CO_2 with reference to that of N_2. The rise in the thermal capacitance due to increase in CO_2 percentage tends to lead to flame cooling and delay in ignition rates and, as a result,

228

the temperature levels are reduced in the regions close to the burners. At downstream regions, this is not the case and the results show similar results for both cases of CO_2%. The change of the reaction model to double-step reactions results in slight reduction in the fluxes which may be attributed to the incomplete combustion of the fuel. Similar results are shown in Figs. 15-16. The presence of CO in the exhaust gases contributes to the lower gas temperature and consequently to lower heat fluxes.
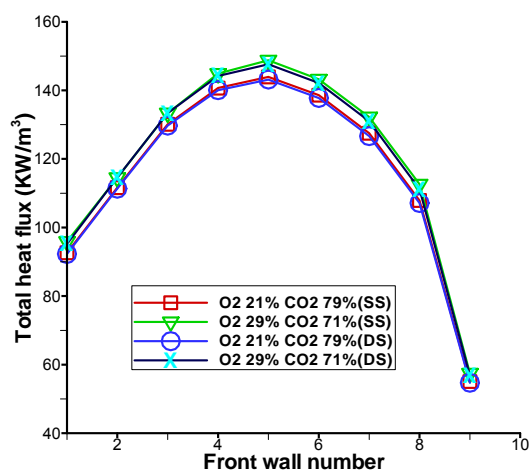

Fig. 15 Total heat flux along the front wall
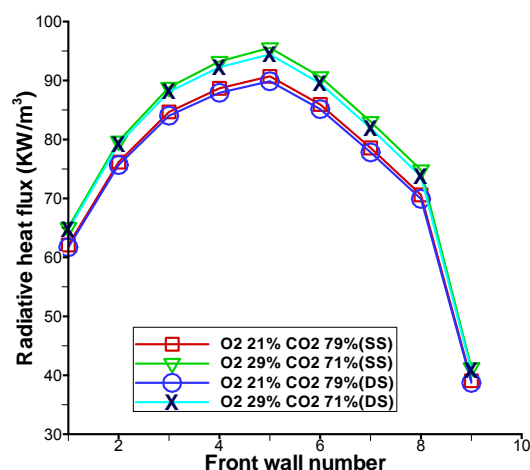
Fig. 16 Radiation heat flux along the front wall

4. CONCLUSIONS

The present research work provides a numerical investigation on the influence of oxygen impurities (dissolved nitrogen in the oxygen supplied for combustion) on the oxy-combustion characteristics temperature and NO_x formation of oxyfuel combustion in an industrial furnace. The effect the number of number of reaction steps on the total and radiation heat transfer is also investigated. Validations of the present computational model were performed by comparing the predicted results with the experimental data and showed a good agreement between predicted and experimental data. The calculations were made for different N_2% of 0, 2, 4 and 6%. Two reaction models are utilized. The first is a one-step and the second is a two-step reaction. The results provide influence of oxygen impurities on the temperature inside the furnace. They also provide influence of N_2 on the maximum temperature, total and thermal NO_x. It is found that the temperature levels are reduced as the carbon dioxide is reduced and nitrogen is introduced. As the nitrogen percent is further increased to 4% and 6% the temperature levels increases slightly.

The influences of the nitrogen percent (oxygen impurities) on the maximum temperature and on the total and thermal NO_x as well as the NO concentration at the exit plane are presented. The results show that the maximum temperature increases with rise in N_2%. As expected, the total NO_x increases with rise in N_2%. The thermal NO_x is shown to increase with N_2% as well. At the exit section, thermal as well as

prompt NO increase as N_2 values have increased.

The results show that increasing the percent of the CO_2 in the CO_2-O_2 side mixture results in a reduction in both the total and radiation heat flux. This is attributed to the high thermal capacity of CO_2 with reference to that of N_2. The rise in the thermal capacitance due to increase in CO_2 percentage tends to lead to flame cooling and delay in ignition rates and, as a result, the temperature levels are reduced in the regions close to the burners. The change of the reaction model to double-step reactions results in slight reduction in the fluxes which may be attributed to the incomplete combustion of the fuel.

ACKNOWLEGEMENTS

REFERENCES

Andersen, J., Rasmussen, C.L., Giselsson, T. and Glarborg, P. (2009), "Global Combustion Mechanisms for Use in CFD Modeling under Oxy-Fuel Conditions", *Energy Fuels*, **23**, 1379-1389.

Andersson, K., Johanson, R., Hjärtstam, S., Johnsson, F. and Leckner, B. (2008), "Radiation intensity of lignite-fired oxy-fuel flames", *Experimental Thermal and Fluid Science*, **33**(1), 67-76.

Andersson, K. and Johnsson, F. (2006), "Radiative properties of a 100 kW oxy-fuel flame experiments and modeling of the Chalmers test facility", *Proceedings of Clearwater Clean Coal Conference*.

Andersson, K., Johanson, R., Johnsson, F. and Leckner, B. (2007), "Radiation intensity of propane-fired oxy-fuel flames: Implications for soot formation", *Energy and Fuels*.

Andersson, K. (2007), "Combustion Tests and Modeling of the Oxy-fuel Process", *2nd Workshop on International Oxy-Combustion Research Network*, Windsor, CT, USA, 25-26, January.

Andersson, K. and Johnsson, F. (2007), "Flame and radiation characteristics of gas-fired O_2/CO_2 combustion", *Fuel*, **86**, 656-668.

Ben-Mansour R., Habib M.A., Nemitallah M.A., Rajhi M. and Suara K.A. (2012), "Characteristics of oxyfuel air fuel combustion in an industrial water tube boiler, HEFAT2012", *Proceedings of the 9th International Conference on Heat Transfer, Fluid Mechanics and Thermodynamics*, Malta, July.

Ben-Mansour R., Habib M.A., Nemitallah M.A., Rajhi M. and Suara K.A. (2014), "Characteristics of oxyfuel air fuel combustion in an industrial water tube boiler", accepted for publication in *Journal of Heat Transfer Engineering*.

Brink, A., Mueller, C., Kilpinen, P. and Hupa, M. (2000), "Possibilities and limitations of the Eddy Break-Up Model", *Combust. Flame*, **123**, 275-279.

Chen, L., Yong, S.Z. and Ghoniem, A.F. (2012), "Oxy-fuel combustion of pulverized

coal: Characterization, fundamentals, stabilization and CFD modeling", *Progress in Energy and Combustion Science*, **38**, 156-214.

Chen, L. and Ghoniem, A.F. (2012), "Simulation of Oxy-Coal Combustion in a 100 kWth Test Facility Using RANS and LES: A Validation Study", Energy Fuels, **26**, 4783-4798. DOI: dx.doi.org/10.1021/ef3006993

Ditaranto, M. and Hals, J. (2007), "Thermo-acoustic instabilities in a CO_2 diluted oxy-fuel combustor", *2nd Workshop on International*, *Oxy-Combustion Research Network*, Windsor, CT, USA, 25-26, January.

Ghoniem, A.F. (2011), "Needs, resources and climate change: Clean and efficient conversion technologies", *Progress in Energy and Combustion Science*, **37**(1), 15-51.

Glarborg, P. and Bentzen, L.L. (2007), "Chemical Effects of a High CO_2 Concentration in Oxy-Fuel Combustion of Methane", *Energy Fuels*, **22**, 291-296.

IPCC Contribution of Working Groups I, II and III to the Fourth Assessment Report of the Intergovernmental Panel on Climate Change (2007), Intergovernmental Panel on Climate Change.

Kakaras, E.A., Koumanakos, A., Doukelis, A., Giannakopoulos, D. and Vorrias, I. (2007), :Oxyfuel boiler design in a lignite-fired power plant", *Fuel*, **86**, 2144-2150.

Liu, F., Becker, H.A. and Bindar, Y. (1998), "A Comparative Study of Radiative Heat Transfer Modeling in as-Fired Furnaces Using the Simple Grey and the Weighted-Sum-of-Grey-Gases Models", *International J. Heat and Mass Transfer*, **41**, 3357-3371.

Magnussen, B.F. and Hjertager B.H. (1976), "On mathematical models of turbulent combustion with special emphasis on soot formation and combustion", *In 16th Symp. (Int'l.) on Combustion*, *The Combustion Institute*.

Modak, A.T. (1979), "Radiation from products of combustion", *Fire Research*, **1**, 339-3361.

Mancini, N.D. and Mitsos, A. (2011), "Ion transport membrane reactors for oxy-combustionepart II: analysis and comparison of alternatives", *Energy*, **36**(8), 4721-4739.

Modak, A.T. (1979), "Radiation from products of combustion", *Fire Research*, **1**, 339-3361.

Raithby, G.D. and Chui, E.H. (1990), "A Finite-Volume Method for Predicting a Radiant Heat Transfer in Enclosures with Participating Media", *J. Heat Transfer*, **112**, 415-423.

Saario, A. and Oksanen, A. (2008), "Comparison of global ammonia chemistry mechanisms in biomass combustion and selective noncatalytic reduction process conditions", *Energy Fuels*, **22**, 297-305.

Shah, M.M. and Christie, M. (2007), "Oxy-fuel combustion using OTM for CO_2 capture from coal power plants", *2nd Workshop on International*, *Oxy-Combustion Research Network*, Windsor, CT, USA, January.

Shaddix, C. (2007), "Coal particle ignition, devolatilisation and char combustion kinetics during oxy-combustion", *2nd Workshop on International*, *Oxy-Combustion Research Network*, Windsor, CT, USA, January.

Smith, T.F., Shen, Z.F. and Friedman, J.N. (1982), "Evaluation of Coefficients for the Weighted Sum of Gray Gases Model", *J. Heat Transfer*, **104**, 602-608.

Versteeg, H.K. and Malalasekera, W. (1995), *An Introduction to Computational Fluid Dynamics*, The Finite Volume Method, Longman Scientific and Technical.

Wall, T.F., Khare, S., Farida, Z. and Liu, Y. (2007), "Ignition of oxy-fuel flames", *2nd Workshop on International Oxy-Combustion Research Network*, Windsor, CT, USA, January.

Westbrook, C.K. and Dryer, F.L. (1981), "Simplified reaction mechanisms for the oxidation of hydrocarbon fuels in flames", *Combust. Sci. Technol.*, **27**, 31-43.

Wilcox, D.C. (2000), *Turbulence Modeling for CFD*, DCW Industries.

Zheng, Y., Fan, J., Ma, Y., Sun, P. and Cen, K. (2000), "Computational modeling of Tangentially Fired Boiler II NO_x Emissions", *Chinese J. Chemical Engineering*, **8**(3), 247-250.